Review of Scientific Instruments

A scalable real-time framework for Thomson scattering analysis: Application to NSTX-U

Cite as: Rev. Sci. Instrum. **90**, 043501 (2019); https://doi.org/10.1063/1.5088248
Submitted: 09 January 2019 . Accepted: 21 March 2019 . Published Online: 10 April 2019

F. M. Laggner, A. Diallo, B. P. LeBlanc, R. Rozenblat, G. Tchilinguirian, E. Kolemen, and NSTX-U Team

Review of Scientific Instruments ARTICLE scitation.org/journal/rsi

A scalable real-time framework for Thomson scattering analysis: Application to NSTX-U

Cite as: Rev. Sci. Instrum. 90, 043501 (2019); doi: 10.1063/1.5088248
Submitted: 9 January 2019 • Accepted: 21 March 2019 •
Published Online: 10 April 2019

F. M. Laggner,[1,2,a] A. Diallo,[1] B. P. LeBlanc,[1] R. Rozenblat,[1] G. Tchilinguirian,[1] E. Kolemen,[2,b] and NSTX-U Team[c]

AFFILIATIONS

[1] Princeton Plasma Physics Laboratory, Princeton, New Jersey 08543, USA
[2] Princeton University, Princeton, New Jersey 08544, USA

[a] Electronic mail: flaggner@princeton.edu
[b] Electronic mail: ekolemen@princeton.edu
[c] See the author list of "NSTX/NSTX-U theory, modeling and analysis results" by S.M. Kaye *et al.*, to be published in Nuclear Fusion: Special Issue on FEC 2018 Summaries and Overviews, https://doi.org/10.1088/1741-4326/ab023a

ABSTRACT

A detailed description of a prototype setup for real-time (RT) Thomson scattering (TS) analysis is presented and implemented in the multi-point Thomson scattering (MPTS) diagnostic system at the National Spherical Torus Experiment Upgrade (NSTX-U). The data acquisition hardware was upgraded with RT capable electronics (RT-analog digital converters and a RT server) that allow for fast digitization of the laser pulse signal of eight radial MPTS channels. In addition, a new TS spectrum analysis software for a rapid calculation of electron temperature (T_e) and electron density (n_e) was developed. Testing of the RT hardware and data analysis software was successfully completed and benchmarked against the standard, post-shot evaluation. Timing tests were performed showing that the end-to-end processing time was reproducibly below 17 ms for the duration of at least 5 s, meeting a 60 Hz deadline by the laser pulse repetition rate over the length of a NSTX-U discharge. The presented RT framework is designed to be scalable in system size, i.e., incorporation of additional radial channels by solely adding additional RT capable hardware. Furthermore, it is scalable in its operation duration and was continuously running for up to 30 min, making it an attractive solution for machines with long discharges such as advanced, non-inductive tokamaks or stellarators.

I. INTRODUCTION

Thomson scattering (TS) is a widely used technique to diagnose hot plasmas. In applications for magnetic confinement fusion (MCF), it is one of the main profile diagnostics since it provides a non-invasive, localized measurement.[1] All larger tokamak as well as stellarator experiments deploy TS diagnostics,[2–10] and also the National Spherical Torus Experiment Upgrade (NSTX-U)[11] is equipped with a multi-point Thomson scattering (MPTS) system.[12] TS is elastic scattering of an electromagnetic wave (a laser pulse) on the free electrons of a plasma. From the scattered light spectrum, the electron temperature (T_e) (spectral broadening) and electron density (n_e) (amplitude) can be inferred. In MCF applications, typically approximations for the TS spectrum, introduced by Selden[13] or by Naito *et al.*,[14] are used to fit the TS measurements. TS diagnostics can be absolutely calibrated using Rayleigh and Raman scattering in gas.[15,16]

There is a growing need for advanced control schemes, such as plasma profile control, which requires real-time (RT) profile measurements as sensors. TS spectra can be analyzed in RT[17–19] owing to an underlying model that allows pre-shot calculation of the TS spectra and a fitting procedure that compares measurement and expectation. At low signal levels, i.e., at low T_e and n_e, the fit accuracy can be improved using advanced data analysis within the Bayesian probability theory.[20,21] Recently, RT T_e data from TS were used for divertor detachment control.[22] Furthermore, the RT equilibrium reconstruction at NSTX-U[23] can be improved by constraining the electron pressure profiles as it was already performed in post-shot equilibrium reconstructions.[24] Ultimately, RT measurements from TS for T_e and n_e, from charge exchange recombination (CER) spectroscopy for ion temperature (T_i) as well as a fast model for the fast ion pressure, such as a neural net[25] or RT capable code,[26] could be combined to attempt a RT reconstruction of kinetic equilibria. As a first step in this effort, the MPTS diagnostic at NSTX-U was equipped with

RT capable data acquisition hardware and a TS spectrum evaluation code was implemented for RT data processing. This provides a prototype framework for RT TS analysis that can be deployed at various TS diagnostics of different MCF experiments.

II. BRIEF DESCRIPTION OF THE NSTX-U MPTS DIAGNOSTIC

At NSTX-U, the MPTS system measures the scattered photon spectrum by means of interference filters and avalanche photo diodes (APDs).[27] A key feature of the setup is the horizontal laser path through the machine's axis, which enables measurements from the low field side (LFS) up to the high field side (HFS).[28] This laser path has been modified to avoid the new, wider center stack of NSTX-U.[29] A similar laser path was also chosen for the TS diagnostic at MAST.[7,30]

Up to now, two Nd:YAG lasers (1064 nm wavelength, nominal pulse energy of 1.6 J, 10 ns pulse width), each with a repetition rate of 30 Hz, are utilized.[28] In the future, the baseline laser pulse repetition rate can be extended to 90 Hz with a new, 30 Hz repetition rate (baseline) laser system. This laser system will feature pulse burst capabilities, enabling a repetition rate of either 10 kHz for 5 ms or a repetition rate of 1 kHz for 50 ms (nominal pulse energy of 1.5 J, 20 ns pulse width).[31]

Spherical mirror optics are deployed to image the laser beam path onto a set of fiber bundles. There is an enhanced packing of channels at the LFS edge to study the pedestal region in detail.[32] Two kinds of polychromator arrangements are currently used to measure the TS spectrum: One with four interference filters and another one using six interference filters. To evaluate n_e from the scattered intensity, Rayleigh as well as Raman calibrations are performed at the beginning and at the end of experimental campaigns.[33]

In summary, the details about the setup and configuration of the MPTS diagnostic at NSTX-U can be found in previously published work.[28,29,32]

Exemplary T_e and n_e profiles of a typical NSTX-U discharge are presented in Fig. 1. Figure 1(a) shows a poloidal cross section of the NSTX-U vessel with an example plasma equilibrium (blue). Furthermore, the laser path (red horizontal line) and the 42 scattering locations (magenta crosses) are presented in Fig. 1(a). The region of the laser path is illustrated in a close up view in Fig. 1(c), and the two vertical arrows indicate the channels that are used to test the RT TS spectrum analysis code (see Secs. III B and V; Figs. 4, 6, and 7). Figure 1(b) presents T_e across the machine radius (R), and Fig. 1(d) shows the corresponding n_e profile. The horizontal bars on the individual measurements indicate the projection of the fiber bundle width on the laser path, which is mapped on R. The dashed vertical lines represent the HFS and LFS parts of the $\psi_N = 0.6$ flux surface (left and right) as well as the location of the magnetic axis (center). To acquire such T_e and n_e profiles in RT, a prototype framework was designed, implemented, and tested for eight radial channels of the MPTS diagnostic.

III. SETUP OF THE REAL TIME MPTS SYSTEM

Having RT TS measurements available gives unique capabilities for plasma control. To enable a RT evaluation of TS spectra, the hardware as well as the software of the MPTS at NSTX-U had to be revised and improved. As a design criterion, the analysis of T_e and n_e should be performed within the baseline laser repetition rate of 60 Hz, i.e., the end-to-end processing time should be smaller than 17 ms. Section III A introduces the selected hardware and describes the RT system layout, while Sec. III B introduces the newly implemented RT TS spectrum evaluation software.

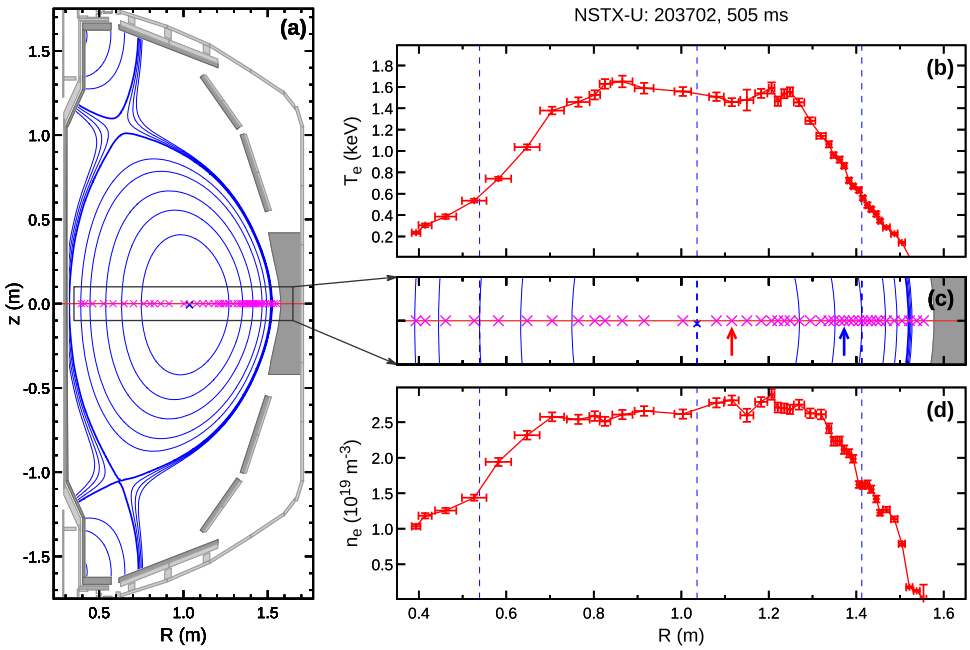

FIG. 1. The channel setup and profiles of the NSTX-U MPTS diagnostic: (a) Poloidal cross section of NSTX-U with the MPTS channel locations, (b) typical electron temperature (T_e) profile, (c) enlarged channel locations, and (d) a typical electron density (n_e) profile. The profiles of T_e and n_e are measured across the full plasma cross section from the LFS to the HFS. The horizontal bars on the profiles indicate the projection of the fiber bundle width on the laser path, mapped to the machine radius (R).

A. Utilized real time capable hardware

As a first step, the data acquisition was exchanged to be RT capable. Here, commercially available SIS3316-250-14 analog digital converters (ADCs) from Struck Innovative Systeme were utilized.[34] These have a digitizing rate of 250 Msamples s^{-1}, two switchable, customized input voltage ranges (0.2 V and 2 V) at 14 bit resolution. The RT readout of these ADCs is done via Gbit Ethernet.

A SuperMicro Real-Time Server[35] is connected to the ADCs and continuously reads out the acquired data. The server has 20 cores, which are clocked at 2.1 GHz, with each having 32 Gb RAM. Multiple cores allow for parallel execution of the TS spectrum analysis of several radial channels. A Flareon Ultra SFN71 Ethernet card from Solarflare[36] and a standard network switch are used to connect the RT server with the ADCs.

As an output interface from the RT server to the NSTX-U plasma control system (PCS), an analog output (AO) card was chosen. It is commercially available and manufactured by General Standards.[37] The model 16AO64 PCIe AO card was selected as it fulfills the system's requirements. This model provides 64 or 32 output channels (depending on the type of operation) with 16 bit resolution and a output rate of 0.5 Msamples s^{-1}.

The upgraded hardware setup is illustrated in Fig. 2. The collected light, emerging from the output of the fiber bundles, enters the polychromator (red wave), which has up to six interference filters with associated APDs and pre-amplifiers. These are connected to the RT-ADC by co-axial cables. The RT-ADCs are wired to the server (RT-MPTS PC) via Ethernet cables. The evaluated data are outputted to the NSTX-U PCS by the AO card that is directly build into the RT-MPTS PC. Furthermore, the evaluated data as well as the acquired raw data are transferred to the MDSplus[38] managed data storage after the plasma discharge.[39] This also allows the standard post-shot TS spectrum analysis.

A major advantage of this system setup is that it works independently of NSTX-U PCS. This is a distinctive feature from another approach of running the RT TS analysis within the PCS.[22] The presented setup does not require any direct interaction between the RT-MPTS PC and the PCS servers, which would require clock synchronization. This enables piggy back RT analysis testing during usual NSTX-U operation without interfering with the NSTX-U PCS. Moreover, running the RT TS spectrum analysis on a separate server does not add any workload on the PCS server, which would be introduced when performing the evaluation within the PCS. The setup allows for a basic error handling via the AO card, when, e.g., data are missing. Furthermore, the system setup is fully modular and could be easily scaled up regarding number of RT-ADCs and computational power by using a more powerful RT-MPTS PC. This would allow for RT usage of more radial channels.

B. Implemented real time software

To perform RT evaluation of the TS spectra, a new software, written in C++11 and optimized for fast and accurate fitting of the TS spectra, was implemented. Figure 3 outlines the main steps of the evaluation work flow. After the initialization, three main evaluation steps are performed to process the acquired TS data to T_e and n_e as well as their corresponding errors. The technical details of each sub step of the evaluation are provided in the following:

- Pre-shot program initialization:
  - Loading of the required calibration data (pre-amplifier and APD gain, Rayleigh and/or Raman calibration), filter transmission, and scattering geometry from the MDSplus data storage
  - Creation of a signal intensity lookup table:
    - Calculation of the expected photon intensities (for a given T_e) at each spectral polychromator channel using the Selden model
    - Considering a T_e range of 0 keV–10 keV and applying a step size of 1 eV
    - Storage in a hash table for fast look-up
  - Initialization of the RT-ADCs
  - Arming of the ADCs and acquisition of data to circular buffer
  - The RT-MPTS system is ready for the next plasma discharge
- Data transfer to a circular buffer:
  - RT data are continuously transferred into circular buffer; the acquired inputs are:
    - Laser Q-switch time sync for each laser (laser ID)
    - Integrating sphere signal (laser energy)
    - Photon intensity signal for the spectral channels of each radial position (photon intens.)
  - Buffer readout is triggered by the laser pulse
  - The detected pulses are fed into the analysis module
- TS spectrum analysis:

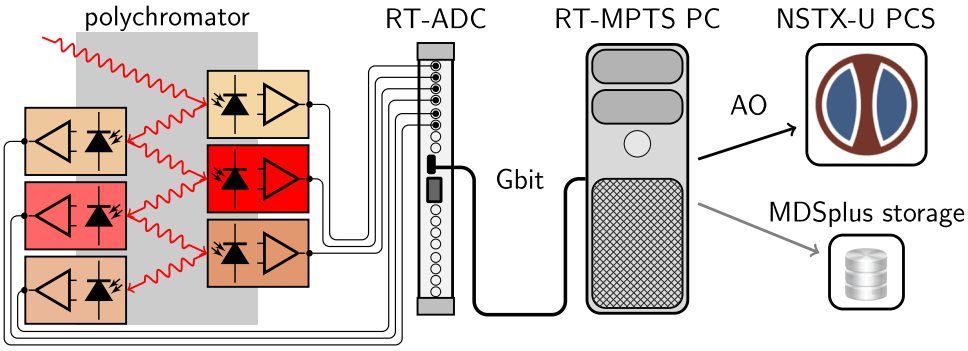

FIG. 2. Sketch of the hardware setup: (left) polychromator with up to six interference filters (not illustrated), APDs, and pre-amplifiers; (middle left) RT-analog digital converter (ADC); (middle right) RT-MPTS PC; and (right) output to the NSTX-U PCS and MDSplus data storage. The polychromator detects the scattered photons, which are digitized by the RT-ADC and analyzed in the RT-MPTS PC. The evaluated T_e and n_e are outputted to the NSTX-U PCS and exported to the MDSplus data storage.

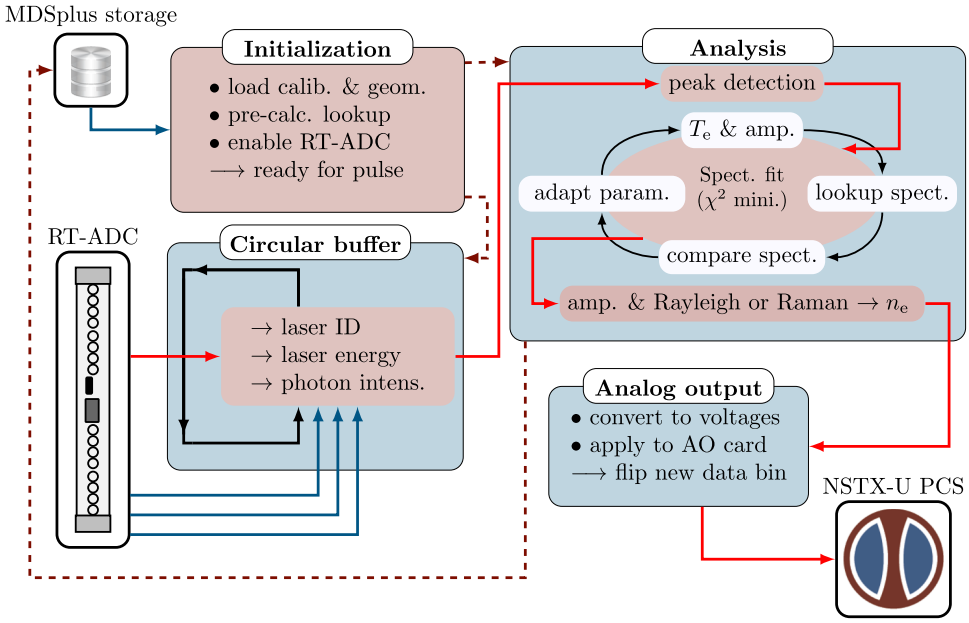

FIG. 3. Sketch of the RT data evaluation work flow: (top left) Initialization, (bottom left) circular buffer for RT data storage, (top right) analysis of the TS spectrum, and (bottom right) analog output (AO) to the NSTX-U PCS. After an initialization sequence, a circular buffer is enabled, which continuously stores data from the RT-ADCs. When the laser is pulsed (red arrow), the buffer is read out and transferred to the analysis module, which calculates T_e and n_e that are then outputted to the NSTX-U PCS.

- Detection of the peak amplitudes of the acquired signal pulses and offset subtractions
- Fitting of the TS spectrum to provide T_e and amplitude including an error estimate:
  - χ^2 minimization of residuals between expected and measured TS spectrum
  - Error calculation of fitted parameters
  - Convergence is achieved after typically 10 iterations (adjustable convergence criteria)
- n_e evaluation using Raman and/or Rayleigh calibration as well as an error estimation
- Passing T_e, T_e error, n_e, and n_e error to AO card
- Post-shot transfer of T_e, T_e error, n_e, and n_e error as well as the detected scattered light pulse raw data to the MDSplus storage

- Output to the NSTX-U PCS:
  - Checking and filtering of evaluated data: Error handling by providing bit indicators for unrealistic analysis results (over-range, under-range, or a general analysis error)
  - Encoding of T_e, T_e error, n_e, and n_e error into output voltages
  - Indication of a new data set to the NSTX-U PCS by modifying a "new data indicator bit"

This evaluation work flow follows a streamlined TS spectrum analysis, which performs more expensive computations already before the plasma discharge. This applies to the evaluation of the Selden model, which is used to calculate the expected photon fluxes at the polychromators' spectral channel. The effective filter transmissions of the polychromator's spectral channels for one core channel [see Fig. 1(c)] are shown in Fig. 4(a). Furthermore, the calculated TS spectra for three different T_e are presented. Combining these spectra with the interference filter transmission as well as detector efficiency and amplification gain gives the expected signal intensity at each spectral channel. The resulting curves of expected intensities

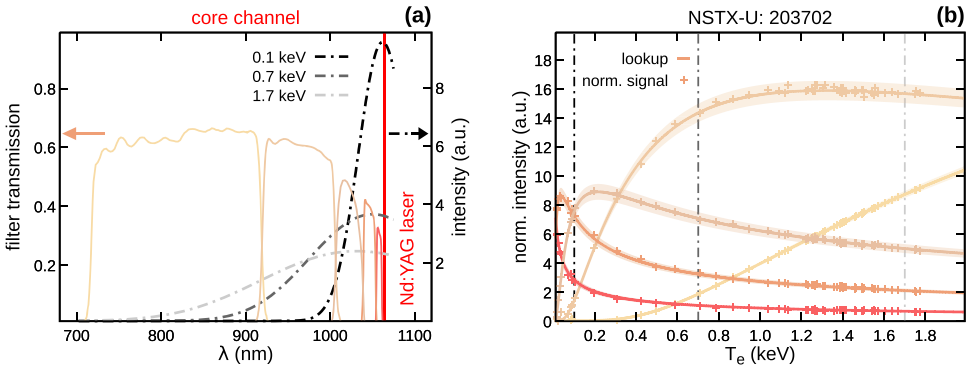

FIG. 4. Creation of an intensity lookup table: (a) Interference filter transmissions of one radial channel and calculated TS spectra and (b) intensities at each spectral channel in dependence of T_e. The intensity lookup table is created by computation of TS spectra for various T_e considering the filter transmission. In the RT analysis, the measured signals are compared to this lookup, identifying T_e that fits best.

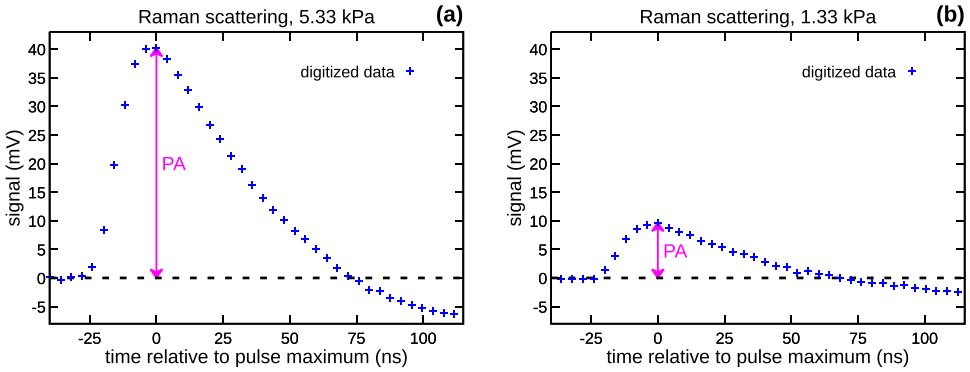

FIG. 5. Raman scattering in nitrogen: (a) at high and (b) low pressure. The 250 MHz RT-ADC enables to finely sample the detected photon pulse. The temporal structure is mostly due to the relatively slow response of the transimpedance pre-amplifier.

in dependence of T_e are presented in Fig. 4(b). During the pre-shot initialization, these curves are evaluated for a T_e range from 0 keV to 10 keV and stored in hash tables for fast look-up. In the RT TS analysis, only a comparison of the expected and measured signal intensity is performed, identifying T_e which has the smallest deviation between measured and expected intensities [see small crosses in Fig. 4(b)]. As presented in Sec. V, a number of tests and benchmarks were successfully performed to prove the RT performance and reliable reproducibility of the evaluated T_e and n_e.

IV. PULSE MEASUREMENT

As an important feature of the new ADCs, the high sampling rate of 250 Msamples s^{-1} enables the acquisition of the temporal evolution of the detected signal. This allows the determination of the background offset before the signal pulse appears. The peak amplitude (PA) can be extracted by searching for the maximum amplitude as the pulse evolves and subtraction of the background offset.

Figure 5 shows examples of digitized signals from Raman scattering in nitrogen. These have been recorded at high (5.33 kPa) and low (1.33 kPa) background pressure. The raw data are indicated in blue, where each cross represents one digitized data point. This reflects a good signal to noise ratio and promises that recorded TS spectra will be well analyzable. For TS spectra, the background offset due to radiation from the plasma is expected to be larger. Nevertheless, the background level is well measured since multiple data points are acquired before the signal pulse appears. Background fluctuations appearing at high frequency during the signal pulse are smoothed out by the response of the utilized transimpedance pre-amplifiers. The pre-amplifiers also cause an artificial undershoot of the signal (to negative voltages) at the end of the signal pulse (cf. Fig. 5). In the future, more advanced fitting of the temporal pulse evolution can be implemented by, e.g., deconvolving the pre-amplifier response function from the detected signal. This can improve the signal to noise ratio at low signal levels, i.e., at low n_e.

In the standard data acquisition, the ADCs are typically triggered at the maximum of the pulse and only this (maximum) amplitude, i.e., the PA, is acquired. Since a similar PA detection is also feasible with the RT-ADCs, a full system integration into the already existing MPTS analysis setup is possible.

V. COMPARISON OF REAL TIME AND POST-SHOT THOMSON SCATTERING COMPUTATION

Extensive tests of the newly developed RT analysis code, including a benchmark against the existing TS spectrum analysis code, were performed. The main difference between the RT and the post-shot analysis is the software implementation and optimization. Besides this, both codes use the Selden model for the TS spectrum and the fitting procedure (χ^2 minimization) is similar. For the benchmark between RT and post-shot analysis code, PA input data, digitized with the standard ADCs, was used. These PA data were fed into the RT spectrum analysis module (Fig. 3), and the output n_e, T_e, as well as the corresponding errors were compared to the standard

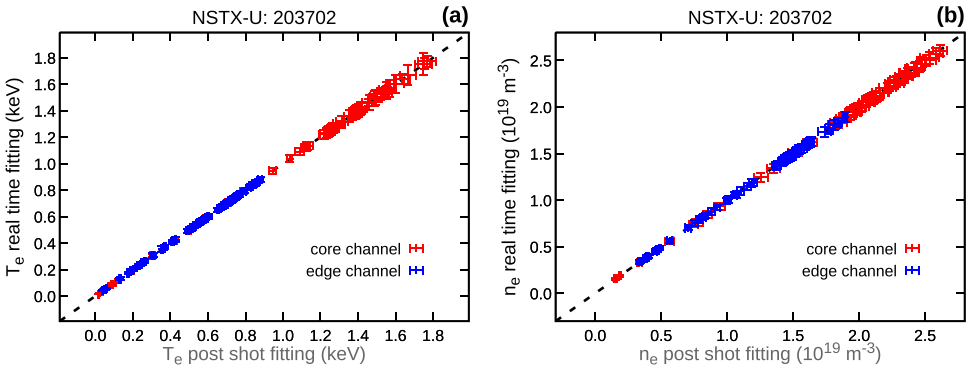

FIG. 6. Fit comparisons of RT and post-shot TS evaluation: (a) electron temperature (T_e) and (b) electron density (n_e) values for a core (red) and an edge (blue) channel. Within the measurement uncertainties, the RT evaluation is capable of reproducing the post-shot evaluated T_e and n_e.

analysis. Figure 6 presents the results of the output comparison for an edge (blue) and a core radial channel (red) of the MPTS diagnostic [see Fig. 1(c)] for all time slices of an exemplary NSTX-U discharge. For T_e [Fig. 6(a)] and n_e [Fig. 6(b)], excellent agreement between both analysis codes is achieved over the covered range. The main advantage of the RT analysis is that it takes less than 2.5 ms to fit the TS spectrum, i.e., to loop through the χ^2 minimization for one time point of one radial channel. This analysis is roughly 10 times faster than the post-shot analysis code, and it can be executed in parallel for several radial channels. The speed up of the calculation time is an essential piece to allow for RT analysis of TS spectra. To achieve a faster solution of the TS spectrum fit, the convergence criteria can be slightly relaxed without drastically changing the outputs of the analysis. The residual χ^2 of the optimization are compared for the RT and the post-shot analysis in Fig. 7. Here, the post-shot and RT analysis are in good agreement, and the small scatter might occur due to the different numerical implementations. Nevertheless, these differences do not cause any systematic differences in the outputted T_e and n_e (cf. Fig. 6).

An end-to-end test of the RT-MPTS system was performed by inputting temporal wave forms of the signals, scaled to provide the actual maximum amplitude of a TS spectrum. Typical signal pulse shapes, as presented in Fig. 5, were utilized and scaled with the measured intensities of a real TS spectrum (digitized with the standard ADCs) and fed in the RT-ADC. These were evaluated by the RT analysis work flow and the calculated T_e and n_e as well as their errors were outputted using the AO card. The timing of the AO was measured relative to the signal input. This test was performed for eight radial channels in parallel and proved that the implemented RT-MPTS system meets a 17 ms end-to-end processing time, i.e., the RT evaluation work flow (Fig. 3) is executed within 17 ms from the triggering of the data readout to T_e and n_e display on the AO card. Furthermore, this processing time was reproducibly achieved over an estimated NSTX-U plasma discharge length of 5 s. The operation time was successfully extended to 30 min to show the system's capability for RT TS analysis of steady state MCF experiments.

This test completes the prototyping of a RT capable framework for the TS analysis. The achieved 17 ms end-to-end processing time should be sufficient for RT control of slowly evolving core plasma parameters. Future optimization aims toward support of a higher laser repetition rate (90 Hz), which requires roughly a reduction in the processing time by 35%. This reduction should be straightforward by upgrading the firmware of the RT ADCs as well as accelerating the RT analysis software. Furthermore, a shorter RT processing time enables the control of edge profile parameters that evolve faster.

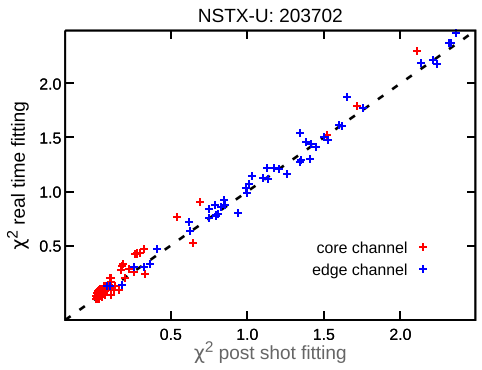

FIG. 7. Comparison of the residual χ^2: RT and post-shot analysis. These have reasonable agreement and do not show any systematic trends.

VI. SUMMARY AND OUTLOOK

The RT data evaluation setup for the MPTS diagnostic at NSTX-U was introduced and successfully tested. ADCs with RT capability and a digitizing rate of 250 Msamples s^{-1} allow to measure the temporal evolution of the APD detectors' signals. In combination with a RT server, the acquired data can be accurately processed and outputted to the NSTX-U PCS. The RT-MPTS system enables RT profile measurements of T_e and n_e as well as estimates of their errors. It will provide the necessary information to perform plasma control using profile information. The main advantage of the presented system layout is that there is a well defined interface between the PCS servers and the RT MPTS server such that both systems operate independently. This minimizes the computational load on the PCS and also allows for piggy back diagnostic operation and optimization during regular plasma operation without interfering with the PCS or with the standard MPTS data evaluation.

Owing to its commercially available hardware and its modular setup, a similar RT system will be deployed at the TS diagnostic of the Large Helical Device (LHD) stellarator.[40,41] For this purpose, the reliable and deterministic operation of the RT TS framework prototype was already demonstrated for 30 min, which is considered to be the duration of the longest plasma discharges. At LHD, the RT system's major application will be to provide RT n_e profiles to track the density evolution during long plasma discharges. This is especially required when electron cyclotron heating (ECH) is continuously applied and n_e is close to the cutoff. In these cases, the microwave beams could be reflected toward the wall. Therefore, this system will provide a density interlock for the ECH system, enabling machine protection from harmful stray radiation.

ACKNOWLEDGMENTS

This work was supported by the U.S. Department of Energy under Grant Nos. DC-AC02-09Ch11466, DE-SC0015878, and DE-SC0015480. NSTX-U is sponsored by the U.S. Department of Energy Office of Science Fusion Energy Sciences. The digital data for this paper can be found following the links from http://arks.princeton.edu/ark:/88435/dsp01nk322h13s.

This report was prepared as an account of work sponsored by an agency of the United States Government. Neither the United States Government nor any agency thereof, nor any of their employees, makes any warranty, express or implied, or assumes any legal liability or responsibility for the accuracy, completeness, or usefulness of any information, apparatus, product, or process disclosed, or represents that its use would not infringe privately owned rights. Reference herein to any specific commercial product, process, or service by trade name, trademark, manufacturer, or otherwise does not necessarily constitute or imply its endorsement, recommendation,

REFERENCES

[1] I. H. Hutchinson, *Principles of Plasma Diagnostics*, 2nd ed. (Cambridge University Press, New York, 2005).
[2] R. Pasqualotto *et al.*, Rev. Sci. Instrum. **75**, 3891 (2004).
[3] D. Johnson *et al.*, Rev. Sci. Instrum. **56**, 1015 (1985).
[4] T. N. Carlstrom *et al.*, Rev. Sci. Instrum. **63**, 4901 (1992).
[5] B. Kurzan *et al.*, Rev. Sci. Instrum. **72**, 1111 (2001).
[6] J. W. Hughes *et al.*, Rev. Sci. Instrum. **72**, 1107 (2001).
[7] R. Scannell *et al.*, Rev. Sci. Instrum. **79**, 10E730 (2008).
[8] K. Narihara *et al.*, Rev. Sci. Instrum. **72**, 1122 (2001).
[9] K. Zhai *et al.*, Rev. Sci. Instrum. **75**, 3900 (2004).
[10] E. Pasch *et al.*, Rev. Sci. Instrum. **87**, 11E729 (2016).
[11] J. E. Menard *et al.*, Nucl. Fusion **52**, 083015 (2012).
[12] D. Johnson *et al.*, Rev. Sci. Instrum. **70**, 776 (1999).
[13] A. C. Selden, Phys. Lett. A **79**, 405 (1980).
[14] O. Naito *et al.*, Phys. Fluids B **5**, 4256 (1993).
[15] E. T. Gerry *et al.*, J. Appl. Phys. **37**, 2715 (1966).
[16] H. Röhr, Phys. Lett. A **60**, 185 (1977).
[17] C. M. Greenfield *et al.*, Rev. Sci. Instrum. **61**, 3286 (1990).
[18] S. Shibaev *et al.*, Fusion Eng. Des. **85**, 683 (2010).
[19] S. Shibaev *et al.*, in *2010 17th IEEE-NPSS Real Time Conference* (IEEE, 2010).
[20] R. Fischer *et al.*, Plasma Phys. Controlled Fusion **45**, 1095 (2003).
[21] S. A. Bozhenkov *et al.*, J. Instrum. **12**, P10004 (2017).
[22] D. Eldon *et al.*, Nucl. Fusion **57**, 066039 (2017).
[23] M. D. Boyer *et al.*, Nucl. Fusion **58**, 036016 (2018).
[24] S. A. Sabbagh *et al.*, Nucl. Fusion **41**, 1601 (2001).
[25] M. D. Boyer *et al.*, Nucl. Fusion **59**(5), 056008 (2019).
[26] M. Weiland *et al.*, Nucl. Fusion **58**, 082032 (2018).
[27] D. W. Johnson *et al.*, Rev. Sci. Instrum. **72**, 1129 (2001).
[28] B. P. LeBlanc *et al.*, Rev. Sci. Instrum. **74**, 1659 (2003).
[29] A. Diallo *et al.*, Rev. Sci. Instrum. **83**, 10D532 (2012).
[30] R. Scannell *et al.*, Rev. Sci. Instrum. **81**, 10D520 (2010).
[31] D. J. D. Hartog *et al.*, J. Instrum. **12**, C10002 (2017).
[32] B. P. LeBlanc *et al.*, Rev. Sci. Instrum. **83**, 10D527 (2012).
[33] B. P. LeBlanc, Rev. Sci. Instrum. **79**, 10E737 (2008).
[34] See http://www.struck.de for detailed information on the utilized RT digitizers.
[35] See http://www.supermicro.com for for customized RT server solutions.
[36] See http://www.solarflare.com for detailed information on the utilized Ethernet card.
[37] See http://www.generalstandards.com for detailed information on high performance bus interfaces.
[38] See http://www.mdsplus.org for a detailed documentation of the utilized data management.
[39] J. A. Stillerman *et al.*, Rev. Sci. Instrum. **68**, 939 (1997).
[40] I. Yamada *et al.*, J. Instrum. **7**, C05007 (2012).
[41] I. Yamada *et al.*, Rev. Sci. Instrum. **87**, 11E531 (2016).